A&A 442, 455–459 (2005)
DOI: 10.1051/0004-6361:20052743

Astronomy & Astrophysics

The large asymmetric HI envelope of the isolated galaxy NGC 864 (CIG 96)⋆

D. Espada[1], A. Bosma[2], L. Verdes-Montenegro[1], E. Athanassoula[2], S. Leon[1], J. Sulentic[3], and M. S. Yun[4]

[1] Instituto de Astrofísica de Andalucía, CSIC, Apdo. 3004, 18080 Granada, Spain
e-mail: daniel@iaa.es
[2] Observatoire de Marseille, 2 Place le Verrier, 13248 Marseille Cedex 4, France
[3] Department of Astronomy, University of Alabama, AL 35487, USA
[4] Department of Astronomy, University of Massachussetts, Amherst, MA 01003, USA

Received 21 January 2005 / Accepted 23 June 2005

ABSTRACT

We present an HI synthesis imaging study of NGC 864 (CIG 96), a spiral galaxy well isolated from similarly sized companions, yet presenting an intriguing asymmetry in its integral HI spectrum. The asymmetry in the HI profile is associated with a strong kinematical perturbation in the gaseous envelope of the galaxy, where at one side the decay of the rotation curve is faster than Keplerian. We detect a small (M(HI) = 5×10^6 $M_\odot$) galaxy with a faint optical counterpart at ~80 kpc projected distance from NGC 864. This galaxy is probably not massive enough to have caused the perturbations in NGC 864. We discuss alternatives, such as the accretion of a gaseous companion at a radial velocity lower than the maximum.

Key words. galaxies: spiral – galaxies: structure – galaxies: kinematics and dynamics – galaxies: evolution – radio lines: galaxies

1. Introduction

The origin of asymmetries in isolated galaxies is not well understood. Are they always induced by the presence of small companions? What is the influence of recent captures, and how long does it take for a parent galaxy to again become axisymmetric afterwards? Could some originate from internal, as yet not well studied, long-lived dynamical instabilities (e.g. Baldwin et al. 1980)? Integral HI spectra provide a powerful statistical approach to this issue since they contain information about both the HI density distribution and the velocity field. We have observed, or compiled from the literature, single-dish 21-cm line spectra for almost 800 galaxies (Espada et al., in preparation) as part of the AMIGA project (Analysis of the interstellar Medium of Isolated GAlaxies; Verdes-Montenegro et al. 2005), which aims to provide a baseline against which environmental effects can be evaluated. We have constructed a complete sample of the most isolated galaxies, starting from the Catalogue of Isolated Galaxies (CIG, Karachentseva 1973; 1050 galaxies), selected on the basis of the distance to the nearest similarly sized galaxies. About 50% of these galaxies show asymmetric HI profiles, consistent with the results from previous work on smaller samples of isolated galaxies (104 galaxies in Haynes et al. 1998; 30 galaxies in Matthews et al. 1998). Surprisingly, other samples of galaxies in denser environments show only slightly larger values of this rate (50–80%, e.g. Swaters et al. 2002; Richter & Sancisi 1994; Sulentic & Arp 1983).

HI synthesis imaging of very isolated galaxies with a highly lopsided HI profile may clarify the origin of these asymmetries. Not only can HI-rich companions be identified, but the presence of tidal features can be revealed, which would trace a past interaction. We have selected from our database a well-defined sample of the most isolated galaxies showing significant asymmetries in their HI profiles (A_n>1.1, see Haynes et al. 1998, for the definition), and mapped them with the VLA[1] in the 21-cm HI line in order to look for signs of external interaction by analyzing in detail the HI distribution and its kinematics.

One of the most interesting galaxies in our VLA sample is NGC 864, number 96 in the CIG catalog, which, as we shall see, shows a peculiar HI envelope in our 21-cm maps. It is classified as SAB(rs)c by de Vaucouleurs et al. (1991). It has an optical size of $4\farcm7 \times 3\farcm5$ and an apparent magnitude m_B = 11.6. It has a very asymmetric HI profile (cf. Fig. 1). The systemic heliocentric velocity that we have measured for this galaxy (see Sect. 3) is 1561.6 km s^{-1}, corresponding to a distance of 17.3 Mpc (H_0 = 75 km s^{-1} Mpc^{-1}) after applying the correction w.r.t. the CMB reference frame. This gives an optical luminosity of 1.1×10^{10} $L_\odot$. The closest galaxy to NGC 864

⋆ Figure 4 is only available in electronic form at http://www.edpsciences.org

[1] The National Radio Astronomy Observatory is a facility of the National Science Fundation Operated under cooperative agreement by Associated Universities, Inc.

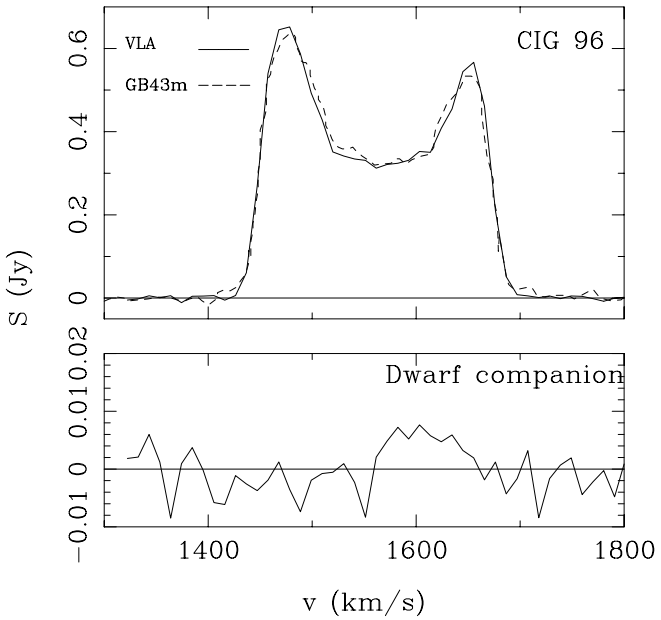

Fig. 1. Comparison of the integrated VLA profile (solid line) and the HI profile obtained by Haynes et al. (1998) at Green Bank 43 m (dots). At the bottom we show the HI profile of the dwarf companion found in the HI map.

at the same redshift is a small companion that we detected in our HI observations (see Sect. 2) with $v_{\rm hel}$ = 1605 km s^{-1}, located at a distance $d \sim 80$ kpc (15′.3) of NGC 864, visible in the POSS2 as a faint object (identified in NED as 2MASX J02162657+0556038 with a reported magnitude of $m_B = 16.38$) with an approximate size of 0′.8 × 0′.6 (physical diameter ∼4 kpc). The other galaxies within a projected radius of $d = 0.5$ Mpc from NGC 864 are fainter by 3 to 7 mag.

2. HI synthesis observations and results

Observations of the 21 cm line for NGC 864 were made with the VLA in its D configuration in July 2004 with 26 antennas. A bandwidth per IF of 3.125 MHz (from 1249.5 to 1895.2 km s^{-1}) was used, in 2IF correlator mode, giving a velocity resolution of 48.8 kHz (10.4 km s^{-1}) for the 64 individual channels after Hanning smoothing. The data were calibrated using the standard VLA procedure in AIPS and were imaged using IMAGR. The average of the line-free channels has been subtracted from all the individual channels. The galaxy was detected between 1436.7 km s^{-1} and 1686.6 km s^{-1}. The synthesized beam was 49″.8 × 46″.2 ($\alpha \times \delta$). The rms noise level achieved after 4 hours is 0.66 mJy/beam. Primary beam correction has been applied to our maps. In Fig. 4 we display the channel maps smoothed to a beam size of 70″.4 × 65″.3, containing the HI emission at the observed radial velocities, from 1426.3 to 1707.4 km s^{-1}. We detect the small companion in the HI map from 1572.0 to 1655.3 km s^{-1}at α(2000.0) = 02$^{\rm h}$16$^{\rm m}$26″.9 and δ(2000.0) = 05°56′24″.0 .

The total spectrum has been obtained by integrating the emission in the individual channel maps (solid line in Fig. 1, top). We have measured a HI content of $M_{\rm HI} = 7.53 \times 10^9\ M_\odot$, in very good agreement with the single dish profile obtained by Haynes et al. (1998, dotted line in Fig. 1, top), showing that there is no loss of flux in the synthesis imaging. The profile of the small companion is shown at the bottom of the same figure. Subtraction of the flux of this dwarf galaxy from the total spectrum will not change its (asymmetric) shape.

In Fig. 2 we show the integrated HI column density distribution of NGC 864 (left) and the HI velocity field (right), both overlaid on a POSS2 red band image, the deepest one we found. These maps have been calculated as follows. The channel maps were smoothed with a Gaussian tapering function, and then non-signal pixels of the maps were blanked out. The channel maps where emission was detected were added up to produce the integrated emission map. The intensity weighted mean radial velocity field has been obtained in a similar way. The small companion mentioned above is clearly seen, together with its faint optical counterpart.

The integrated emission map shows an unresolved HI depression in the center of the galaxy, while the highest column densities are located in a pseudoring structure with a size of ∼90″ × 55″, better seen in the grey scale map shown in Fig. 3. This seems to trace the outer spiral structure of NGC 864, although the spatial resolution of the HI data is too small for a detailed comparison. An arm-like feature seems to join this structure at a second enhancement in the column density distribution. This enhancement has a ring-like shape with an approximate size of 8′.2 × 4′.6 (Figs. 2 and 3), nearly doubling the size of the optical disk. It is more prominent NW and SE of the optical disk and slightly closed to the NE, while undetected to the SW. The receding side of NGC 864 is narrower than the approaching one. The velocity field shows a symmetric pattern of differential rotation in the inner parts ($r \leq 300''$), while the kinematics of the outer parts is strikingly different. The outer isovelocity contours in the northern part show some twisting in the E direction, the last contour being nearly closed as a sign of a flattening rotation curve, and the southern isovelocity contours bend to the south with decreasing values characteristic of a declining rotation curve. The optical disk is reasonably symmetric in both spiral structure and angular extent, except for a slight enhancement of the southern arm, and a minor extension of the optical disk to the SE.

3. Modeling of the galaxy

We have modeled the velocity-field of NGC 864 with a least-square algorithm based on a tilted ring model (Begeman 1987; the ROTCUR task in GIPSY). By this procedure we divided the galaxy into concentric rings, each of them with a width of 20″ along the major axis. The asymmetry of the HI distribution and velocity field in the outer parts lead us to model separately the approaching and the receding part of the galaxy. Points within a sector of ±30° from the minor axis were excluded from the fits. The center position was fixed to the position of the optical center α(2000.0) = 02$^{\rm h}$15$^{\rm m}$27″.6 and δ(2000.0) = 06°00′09″.1 (Leon & Verdes-Montenegro 2003). The systemic velocity of 1561.6 km s^{-1} has been obtained as the central velocity of the HI spectrum at the 20% level. Expansion velocities were set to zero. In a first iteration the position angle, the inclination and rotation velocity have been left free, giving already a very

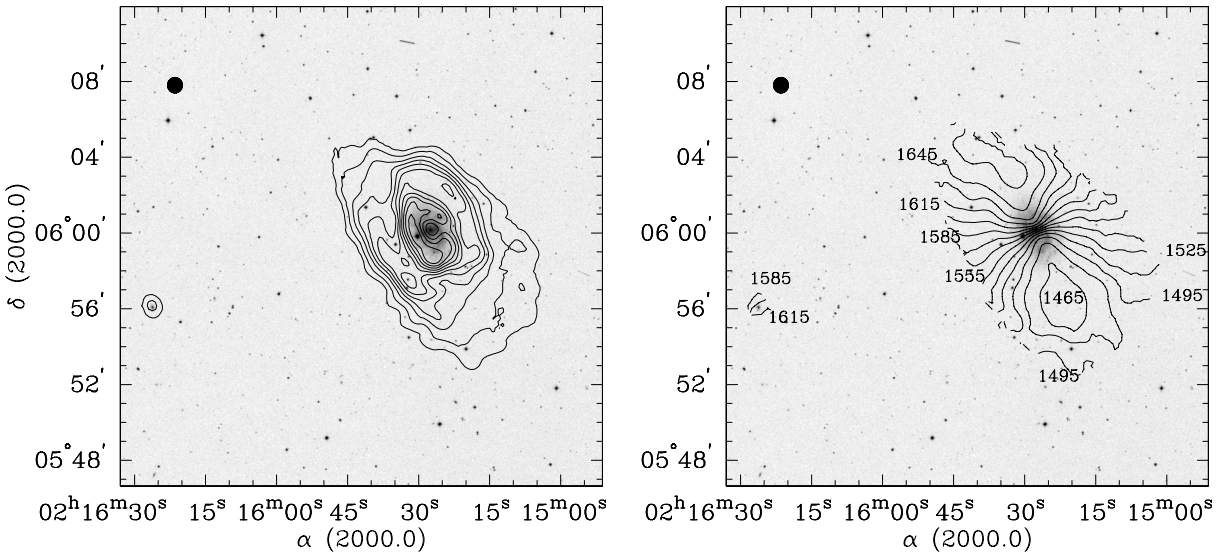

Fig. 2. HI column density distribution (*left*) and velocity field (*right*) of NGC 864 and its companion, superimposed on the optical POSS2 red band image. The contour levels are: 5, 12, 24, 37, 49, 61, 73, 86, 98, 110 and 122 × 10^{20} cm^{-2}. The velocity contours go from 1465 to 1660 km s^{-1} in intervals of 15 km s^{-1}, and are labeled each 30 km s^{-1}. The beam size of 49.″8 × 46.″2 is shown in the upper left of all panels.

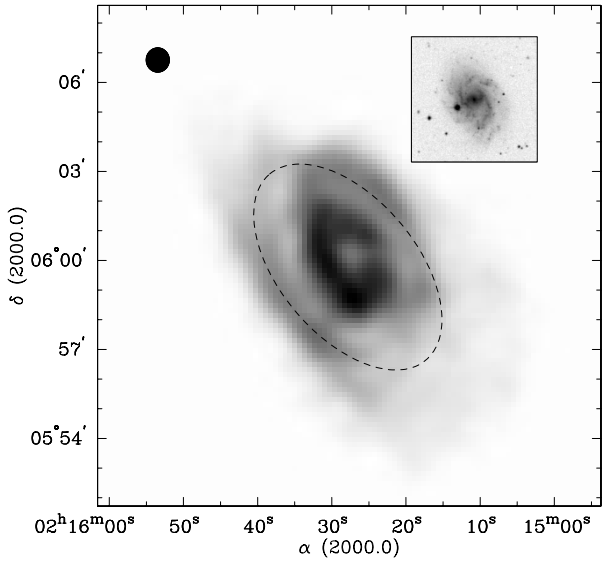

Fig. 3. Grey scale map of the HI column density distribution of NGC 864. Darker regions correspond to higher column densities. The beam size of 49.″8 × 46.″2 is shown in the upper left part. The dashed line defines the approximate location of the pseudoring described in Sect. 2. The insert shows the inner structure of NGC 864.

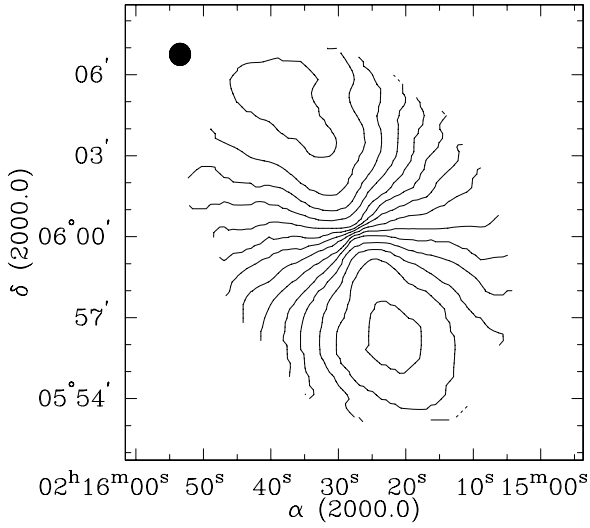

Fig. 5. HI velocity modeled as explained in Sect. 3. The velocity field contours are plotted in the map in km s^{-1} from 1465 to 1660 km s^{-1}, in intervals of 15 km s^{-1}.

satisfactory modeling of the data cube. The derived rotation curve, however, suffers from beam smoothing: since the beam is elongated along the major axis the integration effect biases the radial velocities towards values lower than the true values corresponding to the rotation curve. A second iteration has been performed, this time fixing the radial velocities at slightly higher values in order to correct for beam smearing, and leaving again the position angle and the inclination free. The modeled cubes for the redshifted and blueshifted parts of NGC 864 were combined in a single cube from which a velocity field has been obtained (Fig. 5). It shows a remarkable agreement with the observed one (Fig. 2 right), although not reproducing the asymmetries along the minor axis direction. Deriving the position angle of NGC 864 from our modeling for $r \leq 300''$ we obtain a mean value of 23° ± 3, in very good agreement with the optical disk orientation. The inclination obtained as the mean between the receding and approaching sides is 43° ± 2, which is consistent to the value given by Tully (1988) of 45°. The modelled inclinations for both sides are almost constant and their values are always close to the mean. The major axis twists both in the northern and southern part of NGC 864, although is more pronounced to the north. There it starts at $r \sim 240''$ at nearly the edge of the optical disk, reaching a position angle of 39°. In the southern part it starts at $r \sim 360''$ going up to 31°. In Fig. 6 we compare the position-velocity cut at 23° for the

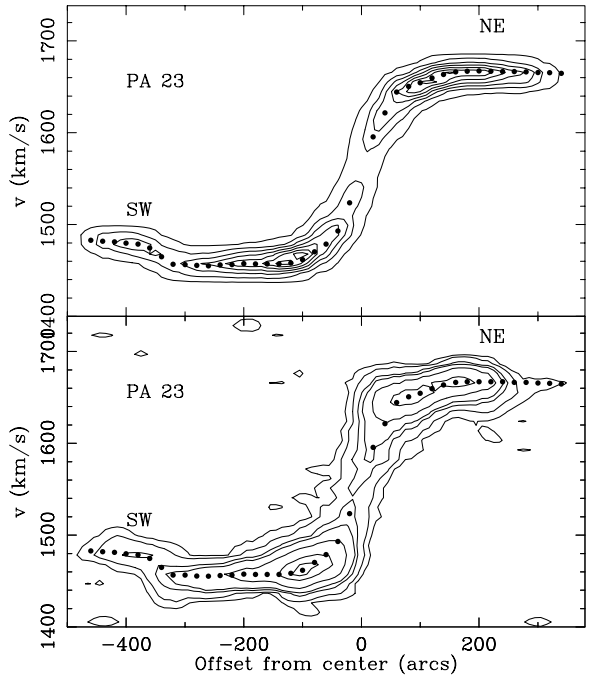

Fig. 6. Position velocity along PA = 23° for the model (*top*), and for the observations (*bottom*). The projected rotation curve is also plotted (dots).

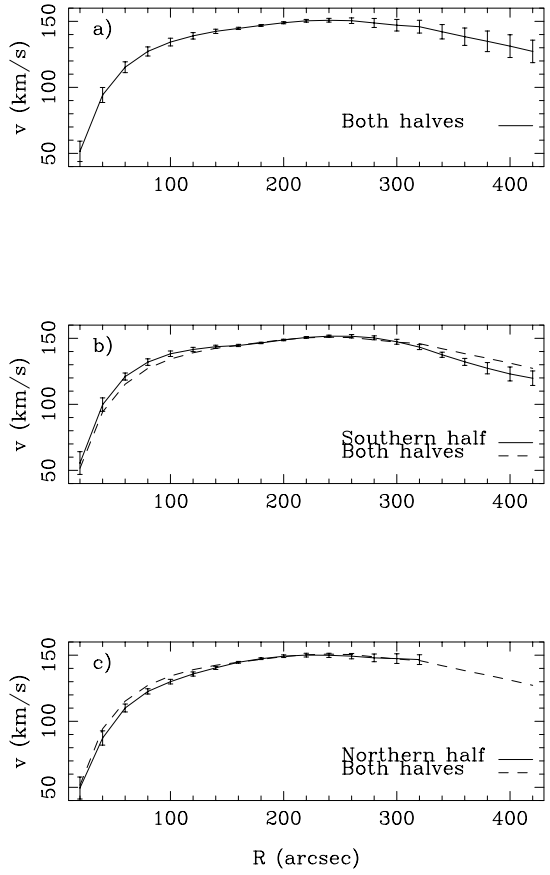

Fig. 7. Rotation curves of NGC 864 considering: **a)** both the receding and approaching regions; **b)** the approaching half (southern region) and **c)** the receding half only (northern region). The dashed line represents the rotation curve in a) without error bars.

modeled (top) and observed (bottom) cube. Again the observations are very well reproduced. The plot also shows the projected rotation curve used. This figure contains the essential peculiarities of NGC 864: asymmetric HI distribution and kinematics, with a noticeable drop in rotation velocities. We note that the blueshifted part of the observed position-velocity diagram shows a faster than keplerian drop in the velocity of NGC 864, with a trend to reach $r^{-0.5}$ values at larger radii, that should of course be explained by non-circular motions and/or projection effects. Such a phenomenon is extremely rare in HI envelopes.

4. Discussion and conclusions

Our results for NGC 864 have wider implications:

a) The integral HI profile is symmetric in velocity, but asymmetric in intensity. Yet the 2D-kinematics of NGC 864 show large scale asymmetries: there is a kinematic warp, and in the southern part there is an abrupt decline of the rotation velocity, as is evident in Fig. 6. The atomic gas here looks like a kinematically detached clump, evident as a secondary peak in the position velocity cut at radii ∼400″ to the SW. This region has a physical extent of around $3' \times 4'$ in the major axis and minor axis directions, respectively. Clearly a simple integrated profile analysis will conclude that the central parts of NGC 864 are roughly symmetric, with a value of ΔV_{20} correlated with the luminosity of the galaxy, since it falls on the Tully-Fisher relation. It is the outer parts which are surprisingly asymmetric, but since the radial velocities in the approaching side are closer to the systemic velocity than those in the central parts, the asymmetry only manifests itself in a higher amplitude of the blueshifted horn of the HI profile.

b) The outer HI envelope is large, massive, very asymmetric and presents much structure. Its HI mass is about $4.5 \times 10^9\ M_\odot$, and the HI mass associated with the steep drop of the rotation curve is about $2.3 \times 10^8\ M_\odot$. No optical counterpart is found associated with the perturbed atomic gas. Warped HI envelopes are common around spirals, but few have as much structure and asymmetries as the one reported here.

c) The galaxy is isolated with respect to similarly sized galaxies by a rather strict criterion. Yet there are 5 small companions within a projected distance of 500 kpc. The closest one, detected in our maps, has a dimensionless gravitational interaction strength (Dahari 1984) of 4×10^{-4}, while for the others this parameter ranges from 1×10^{-5} to 8×10^{-7}. They are hence too small in mass to have caused the strong perturbations in the outer envelope of NGC 864. A similar conclusion follows from considerations about spiral forcing by companions (cf. Athanassoula 1984).

We have considered several possibilities to explain the origin of these HI asymmetries. A self-induced perturbation seems highly unlikely: while the pseudoring is a very standard feature, the outer HI ring-like structure is too large to be a broken resonance ring, since the outer Lindblad resonance is usually located at slightly over 2 times the end of the bar

(Athanassoula et al. 1982). An external perturbation by a companion, which could have interacted or even been accreted, seems likely to have caused the SW clump and the outer ring-like structure. However, we can exclude an encounter with a large pericenter distance since this would necessitate a massive companion, which is simply not there. A small companion would have to come very near NGC 864 or, even better, go through it, but a central, or near-central, passage will (cf. Athanassoula et al. 1997; Berentzen et al. 2003) yield results that do not match at all the morphology of NGC 864. The alternative left is that the companion crossed the equatorial plane of the target at an intermediate distance, e.g. just outside the optical disc and still within the extended HI disc. Such a passage could have induced the warp, and if the intruder was a loosely bound gas rich dwarf, its gas could have contributed to the SW clump, which has a similar gas mass, while its stars and dark matter could have dispersed. In order to test this interpretation and explain the form of the ring-like density enhancement, the mass of the excess gas and the velocity perturbations, full blown selfconsistent simulations including both gas and stars are necessary, but beyond the scope of the present paper.

Acknowledgements. D.E., S.L. and L.V.M. are partially supported by DGI Grant AYA 2002-03338 and Junta de Andalucía TIC-114 (Spain). L.V.-M. acknowledges the hospitality of the Observatoire de Marseille. We used the NASA/IPAC Extragalactic Database (NED), operated by the Jet Propulsion Laboratory, California Institute of Technology, under contract with the National Aeronautics and Space Administration.

References

Athanassoula, E. 1984, Phys. Rep., 114, 321
Athanassoula, E., Bosma, A., Crézé, M., & Schwarz, M. P. 1982, A&A, 107, 101
Athanassoula, E., Puerari, I., & Bosma, A. 1997, MNRAS, 286, 284
Baldwin, J. E., Lynden-Bell, D., & Sancisi, R. 1980, MNRAS, 193, 313
Begeman, K. 1987, Ph.D. Thesis, University of Groningen
Berentzen, I., Athanassoula, E., Heller, C. H., & Fricke, K. J. 2003, MNRAS, 341, 343
Dahari, O. 1984, AJ, 89, 966
De Vaucouleurs, G., De Vaucouleurs, A., Corwin, H. G., et al. 1991, Third Reference Catalog of Bright Galaxies (Berlin: Springer), AJ, 95, 697
Haynes, M. P., van Zee, L., Hogg, D. E., Roberts, M. S., & Maddalena, R. J. 1998, AJ, 115, 62
Karachentseva, V. E. 1973, Comm. Spec. Ap. Obs., USSR, 8, 1
Leon, S., & Verdes-Montenegro, L. 2003, A&A, 411, 391
Matthews, L. D., van Driel, W., & Gallagher, J. S., III 1998, AJ, 116, 1169
Richter, O. G., & Sancisi, R. 1994, A&A, 290, 9
Sulentic, J. W., & Arp, H. 1983, AJ, 88, 489
Swaters, R. A., van Albada, T. S., van der Hulst, J. M., & Sancisi, R. 2002, A&A, 390, 829
Tully, R. B. 1988, Nearby Galaxies Catalog (Cambridge: Cambridge Univ. Press)
Verdes-Montenegro, L., Sulentic, J., Lisenfeld, U., et al. 2005, A&A, in press

Online Material

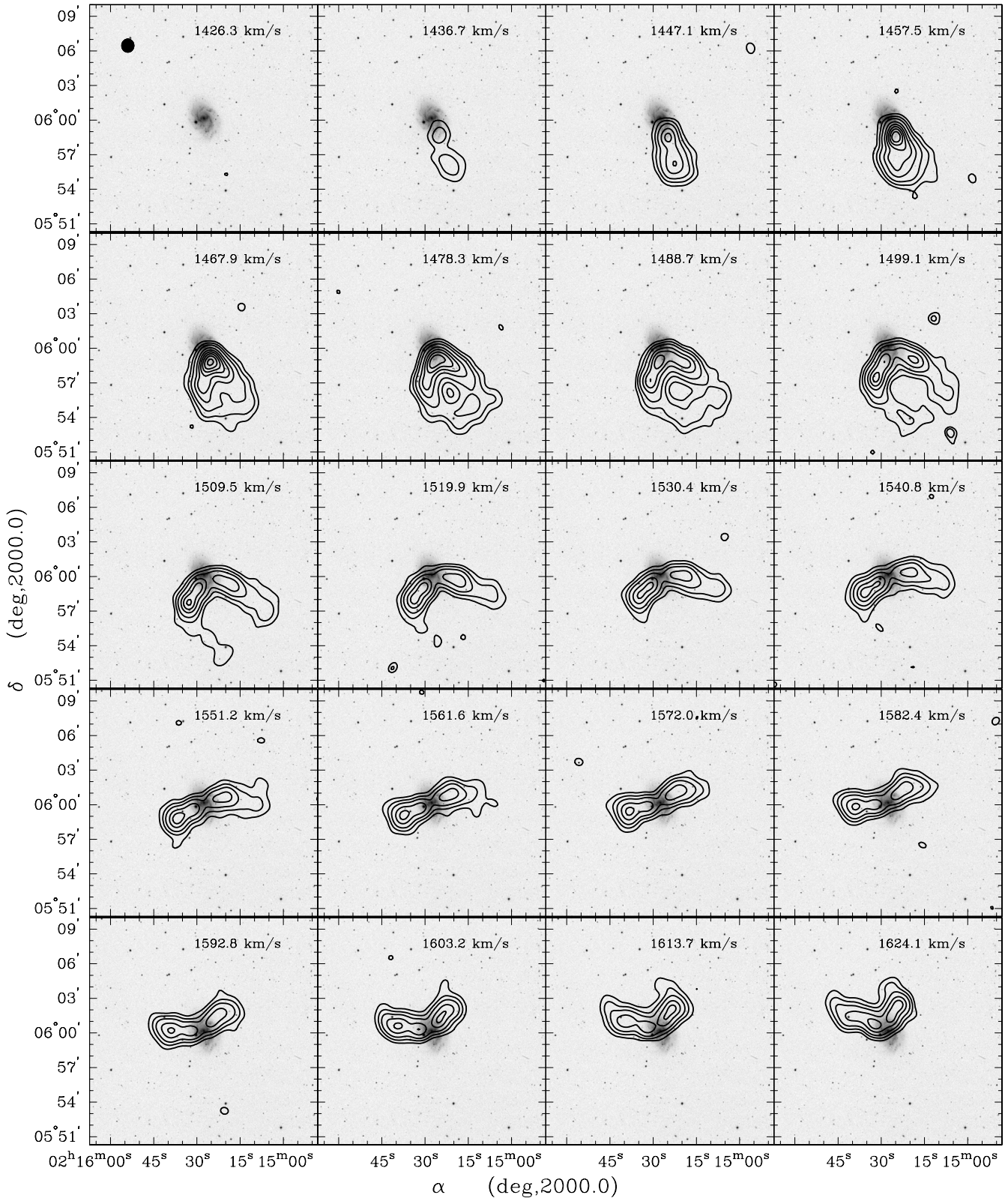

Fig. 4. HI channel plots superimposed on the optical POSS2 red band image. The beam size of 70.″4 × 65.″3 is shown in *the upper left part*. The contour levels are: 3, 8, 16, 32, 48, 64, 80 and 96 mJy/beam.

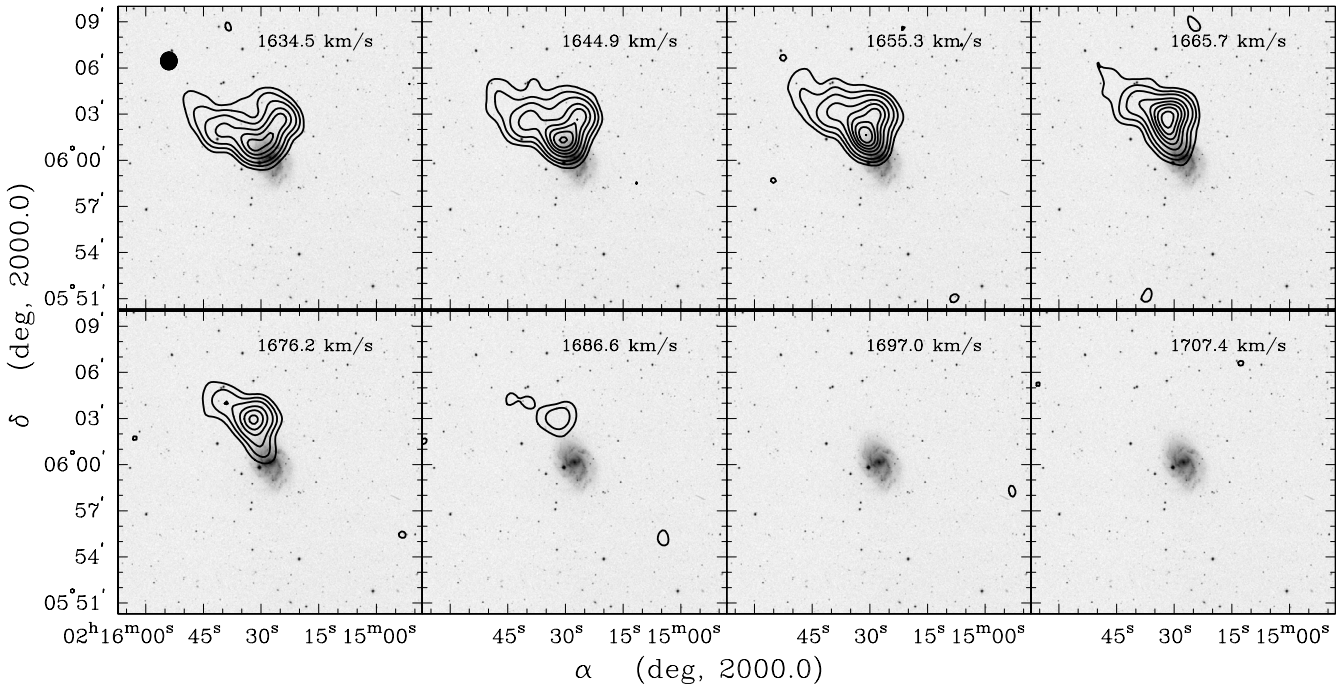

Fig. 4. continued.